nature neuroscience

Identification of distinct telencephalic progenitor pools for neuronal diversity in the amygdala

Tsutomu Hirata[1], Peijun Li[2], Guillermo M Lanuza[3], Laura A Cocas[1,4], Molly M Huntsman[2] & Joshua G Corbin[1]

The development of the amygdala, a central structure of the limbic system, remains poorly understood. We found that two spatially distinct and early-specified telencephalic progenitor pools marked by the homeodomain transcription factor *Dbx1* are major sources of neuronal cell diversity in the mature mouse amygdala. We found that *Dbx1*-positive cells of the ventral pallium generate the excitatory neurons of the basolateral complex and cortical amygdala nuclei. Moreover, *Dbx1*-derived cells comprise a previously unknown migratory stream that emanates from the preoptic area (POA), a ventral telencephalic domain adjacent to the diencephalic border. The *Dbx1*-positive, POA-derived population migrated specifically to the amygdala and, as defined by both immunochemical and electrophysiological criteria, generated a unique subclass of inhibitory neurons in the medial amygdala nucleus. Thus, this POA-derived population represents a previously unknown progenitor pool dedicated to the limbic system.

The broad function of the amygdala is to integrate and process information from external stimuli and coordinate appropriate behavioral outputs[1–3]. These complex functions are differentially regulated by the 11–15 distinct functional subnuclei of the amygdala, which make numerous connections with multiple cortical and subcortical brain regions. These subnuclei can also be grouped together according to a variety of criteria, including connectivity, function and neuronal diversity. The most studied of these nuclear groups is the basolateral complex, which comprises the lateral, basolateral and basomedial nuclei. The prime function of the basolateral complex is the processing and storage of information with emotional salience, particularly fear. In contrast, the function of the medial nucleus, via connections with the olfactory bulb and hypothalamus, is to integrate chemosensory and hormonal signals to control social, reproductive, feeding and defensive behaviors. The importance of the amygdala in human behavior is shown by the fact that amygdala dysfunction is a key component of numerous prevalent human disorders such as autism, autism spectrum disorders and stress-related psychological disorders such as post-traumatic stress disorder[4–6]. Thus, unraveling the development of this complex structure is an important goal with potential translational applications.

The unique connectivity and complex nuclear organization of the amygdala sets it apart from all other telencephalic structures, most notably from laminar brain structures such as the cerebral cortex and hippocampus. In addition to classification according to functional criteria, individual amygdala nuclei have also been grouped on the basis of whether their principal output neurons are excitatory (glutamatergic) or inhibitory (GABAergic)[1–3]. Major excitatory nuclei include the basolateral complex and cortical nuclei and major inhibitory nuclei include the central and medial nuclei. Although differing in their neuronal composition, both excitatory and inhibitory nuclei are also comprised of a variety of functionally diverse interneuron subtypes that are essential for the proper regulation of the firing of the output neurons. The coordinated development of these neuronal cell types during embryogenesis is essential for the formation of complex amygdala circuitry. However, despite its central role in normal and abnormal brain function and behavior, little is currently known regarding how neuronal cell diversity is generated in the amygdala.

In this study, we examined the contribution of progenitor cells to excitatory and inhibitory cell diversity in the mature amygdala. Previous work from our laboratory, as well as others, has indicated that the pallial-subpallial boundary (PSB) of the telencephalon, the region of the telencephalon where pallial (for example, high *Pax6* and *Neurog2*) and subpallial (for example, *Gsx2* and *Dlx1/2*) gene expression abuts, is a major source of amygdala neural progenitors[7–10]. In addition to expressing regional markers, the pallial and subpallial aspects of the PSB express a unique combination of genes that includes the homeodomain transcription factor *Dbx1*, which marks the ventral pallial progenitors of the PSB[9,11–13]. Outside of the PSB, *Dbx1* is expressed in other progenitor regions of the developing telencephalon such as the POA and septum. Although a previous study has revealed that *Dbx1*-derived progenitors, specifically from the PSB and septum, contribute early-born Cajal-Retzius cells to the piriform and cerebral cortices[11], the question of whether this progenitor population contributes to amygdala cell diversity remains unexplored.

Using a combination of mouse genetic fate mapping, *in vitro* migratory assays and electrophysiological approaches, we found that the ventral pallial *Dbx1*-positive progenitor pool is a source of

[1]Center for Neuroscience Research, Children's National Medical Center, 111 Michigan Avenue, NW, Suite 645, Washington, DC 20010, USA. [2]Department of Pharmacology, Georgetown University School of Medicine, 3900 Reservoir Rd., NW, Washington, DC 20057, USA. [3]Fundación Instituto Leloir, Av. Patricias Argentinas 435, Buenos Aires 1405, Argentina. [4]Interdisciplinary Program in Neuroscience, Georgetown University School of Medicine, 3900 Reservoir Rd., NW, Washington, DC 20057, USA. Correspondence should be addressed to J.G.C. (jcorbin@cnmcresearch.org).

Received 16 October 2008; accepted 13 November 2008; published online 11 January 2009; doi:10.1038/nn.2241

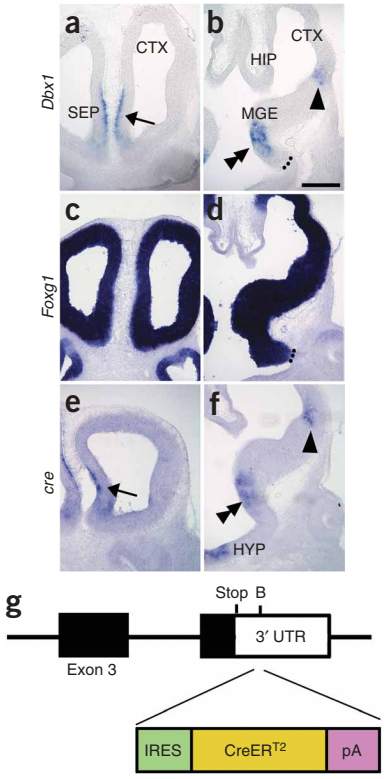

Figure 1 Expression of *Dbx1* and knock-in approach. (**a**–**f**) Expression of *Dbx1* (**a**,**b**) and *Foxg1* (**c**,**d**) in wild-type embryos and *cre* (**e**,**f**) in *Dbx1*$^{+/CreERT2}$ knock-in embryos at E11.5 is shown at rostral and caudal levels in coronal sections. *Dbx1* was expressed in the septum (**a**, arrow), the ventral pallium (**b**, arrowhead) and the POA (**b**, double arrowhead). *Foxg1* expression delineated the telencephalon from the diencephalon (**c**,**d**). Dotted lines in **b** and **d** indicate the telencephalic-diencephalic border. *cre* expression recapitulated *Dbx1* expression in the septum (**e**, arrow), the ventral pallium (**f**, arrowhead) and the POA (**f**, double arrowhead). (**g**) Schematic of the knock-in approach in which an IRES-CreER^{T2} cassette was inserted into the 3′ UTR of the fourth exon of *Dbx1*. CTX, cerebral cortex; HIP, hippocampus; HYP, hypothalamus; MGE, medial ganglionic eminence; SEP, septum. Note that embryonic anatomy is taken from ref. 37. Scale bar represents 250 μm.

excitatory neurons in the basolateral complex and cortical nuclei, the primary excitatory output nuclei of the amygdala. In addition, we uncovered a previously unknown migratory route, termed the POA-amygdala migratory stream (PAS), which is composed of *Dbx1*-derived cells from the POA to the emerging amygdala. Our electrophysiological analysis indicated that this migratory population gives rise to a markedly restricted functional subclass of inhibitory neurons specifically in the mature medial amygdala nucleus. These inhibitory neurons are also characterized by their unique morphology and expression of inhibitory neuronal markers, such as neuronal nitric oxide synthase (nNOS), which, together with their electrophysiological characteristics, distinguishes them from other known telencephalic inhibitory neuron subclasses. Thus, our data reveal that spatially distinct telencephalic *Dbx1*-positive progenitor pools are major sources of neuronal diversity for distinct nuclei of the mature amygdala and indicate the presence of a previously unknown relationship between genetically marked progenitor pools and their limbic system fate.

RESULTS

Expression of *Dbx1* and generation of CreER^{T2} knock-in mice

Previous studies have revealed that the PSB is comprised of progenitors from the ventral pallium and dorsal LGE (dLGE) and is the source of the lateral cortical stream (LCS) migratory route to the amygdala[7,8,13]. Expression of *Dbx1* marked ventral pallial progenitors as well as the developing septum and POA from embryonic day (E) 9.5 to E14.5 (**Fig. 1a**,**b** and data not shown)[9,12]. The *Dbx1*-expressing region in the POA was also positive for *Foxg1* (ref. 14), indicating that this population is of telencephalic, rather than the diencephalic, origin (**Fig. 1c**,**d**).

To examine the fate of *Dbx1*-positive cells, we used a genetic fate-mapping approach in which an IRES-CreER^{T2} cassette was inserted into the 3′ UTR region of the *Dbx1* gene. This strategy allows for the indelible marking of genetically defined progenitor populations from embryogenesis to adulthood and is thus a powerful tool for tracking the fate of specific progenitor populations[15,16]. Our analysis of *Dbx1*$^{+/CreERT2}$ embryos revealed that *cre* was expressed in the same pattern as *Dbx1* (**Fig. 1e**,**f** and data not shown) and the insertion of an IRES-CreER^{T2} cassette into the 3′ UTR of the *Dbx1* locus (**Fig. 1g**) did not appear to interfere with normal *Dbx1* expression (**Supplementary Fig. 1** online)[11].

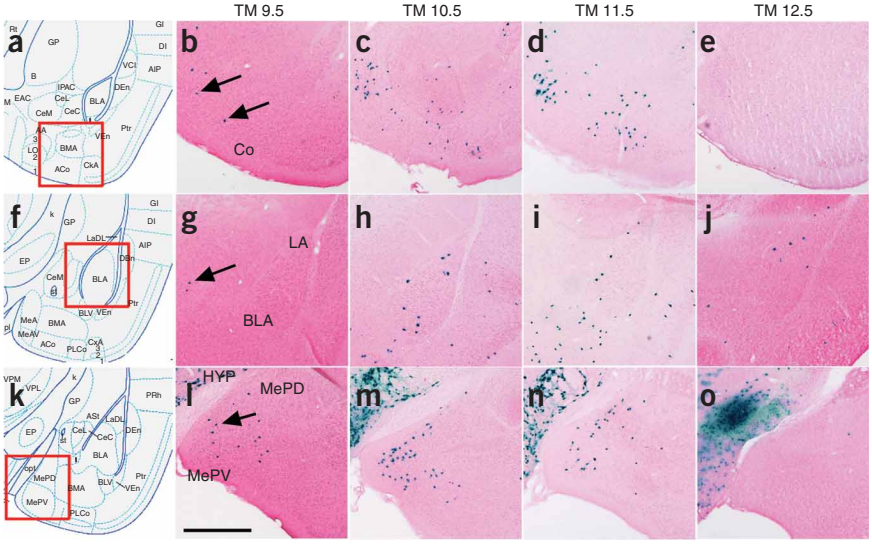

Figure 2 *Dbx1*-derived cells in the postnatal amygdala. (**a**–**o**) β-galactosidase staining of coronal sections from *Dbx1*$^{+/CreERT2}$;*R26R-LacZ* brains at P21 revealed numerous recombined β-galactosidase–positive cells in the amygdala. Distribution of recombined cells from tamoxifen administration at E9.5 (**b**,**g**,**l**), E10.5 (**c**,**h**,**m**), E11.5 (**d**,**i**,**n**) or E12.5 (**e**,**j**,**o**) are shown. Boxed areas in schematics (**a**,**f**,**k**) indicate the region of the amygdala shown in each panel. E9.5 tamoxifen delivery resulted in recombined cells in the cortical and medial nuclei (**b**,**g**,**l**, arrows), but not in the lateral and basolateral nuclei. In addition to the cortical and medial nuclei, tamoxifen delivery at E10.5 (**c**,**h**,**m**) or E11.5 (**d**,**i**,**n**) resulted in recombined cells in the lateral and basolateral nuclei. Tamoxifen delivery at E12.5 resulted in recombined cells in the lateral and basolateral nuclei only (**e**,**j**,**o**). BLA, basolateral nucleus; Co, cortical nucleus; LA, lateral nucleus; MePD, medial nucleus posterior dorsal; MePV, medial nucleus posterior ventral. Scale bar represents 500 μm.

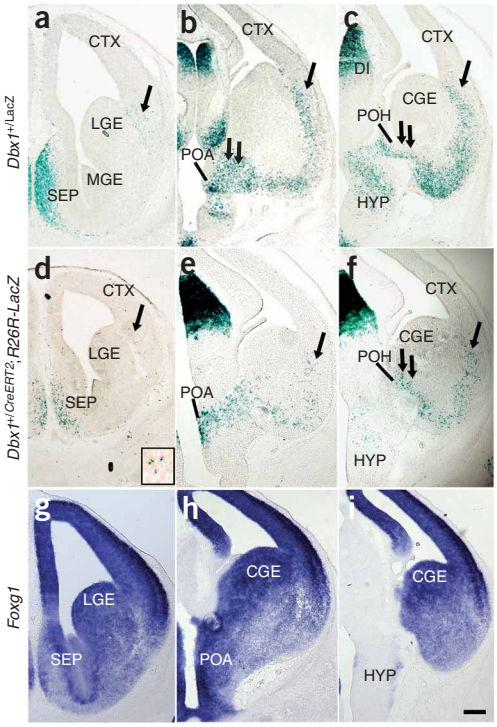

Figure 3 *Dbx1*-derived cells in the developing basal telencephalon. (**a**–**f**) β-galactosidase staining of coronal sections of E13.5 $Dbx1^{+/LacZ}$ knock-in (**a**–**c**) and $Dbx1^{+/CreERT2}$;*R26R-LacZ* embryos (**d**–**f**) revealed putative migrating cells to the region of the developing amygdala. β-galactosidase–positive cells are shown along the both LCS (**a**–**f**, single arrow, inset in **d** shows a higher magnification of β-galactosidase–positive cells in the LCS) and the putative PAS (**b**,**c**,**e**,**f**, double arrows). (**g**–**i**) *Foxg1* expression in corresponding sections in $Dbx1^{+/CreERT2}$;*R26R-LacZ* knock-in embryos indicated that *Dbx1*-derived cells distributed along PAS were located in the telencephalon. Note the relative paucity of β-galactosidase–positive cells in the ganglionic eminences and the developing cerebral cortex. CGE, caudal ganglionic eminence; DI, diencephalon; LGE, lateral ganglionic eminence; POA, preoptic area; POH, preopto-hypothalamic region. Scale bar represents 250 μm.

Dbx1-derived cells contribute to the amygdala

To examine the fate of *Dbx1*-derived cells in the amygdala, we crossed $Dbx1^{+/CreERT2}$ mice with *R26R-LacZ* reporter animals that permanently express β-galactosidase on Cre-induced recombination[17]. The fusion of Cre to the tamoxifen-sensitive estrogen receptor (ER^{T2}) allows Cre translocation to the nucleus to be controlled by the administration of tamoxifen, with recombination typically occurring 6–12 h after tamoxifen delivery[18]. We administered tamoxifen to pregnant dams at E9.5, E10.5, E11.5 or E12.5 and examined the distribution of β-galactosidase–labeled cells at postnatal day (P) 21 in both the telencephalon and diencephalon (**Fig. 2** and **Supplementary Fig. 2** online). Tamoxifen administration at E9.5 resulted in the appearance of recombined cells mainly in the medial amygdala nucleus, with only a few recombined cells being observed in the cortical nucleus and none in the basolateral complex (lateral, basolateral and basomedial nuclei) (**Fig. 2b**,**g**,**l**). However, tamoxifen administration 1 d later at E10.5 (**Fig. 2c**,**h**,**m**) or 2 d later at E11.5 (**Fig. 2d**,**i**,**n**) resulted in the appearance of recombined cells in the basolateral complex and cortical and medial nuclei. In contrast, tamoxifen delivery at E12.5 resulted in recombined cells appearing primarily in the basolateral complex, with only a few recombined cells being detected in the medial and cortical nuclei (**Fig. 2e**,**j**,**o**) These data indicate that *Dbx1*-positive progenitors generate cells that are destined for the amygdala in two waves: medial and cortical nuclei cells first (starting at approximately E10.0), followed approximately 1 d later by cells of the basolateral complex.

Because *Dbx1* is expressed in multiple domains in the embryonic telencephalon, we examined the origins of *Dbx1*-derived cells by analyzing patterns of putative migratory pathways in two sets of transgenic mice in which *Dbx1*-positive progenitors and their progeny were marked: previously generated $Dbx1^{+/LacZ}$ mice, in which LacZ was knocked into the *Dbx1* locus[19], and the $Dbx1^{+/CreERT2}$;*R26R-LacZ* mice described above (**Fig. 3**). Analysis of $Dbx1^{+/LacZ}$ embryos at E13.5 revealed cohorts of β-galactosidase–positive cells along the LCS migratory route from the ventral pallium to the basal telencephalon (**Fig. 3a**,**b**). In addition, we detected a large putative migratory route (the PAS) between the POA and the developing amygdala (**Fig. 3b**,**c**).

Similar patterns of putatively migrating β-galactosidase–positive recombined cells were observed in $Dbx1^{+/CreERT2}$;*R26R-LacZ* embryos (**Fig. 3d–f**). As revealed by *Foxg1* expression, the PAS appeared to originate in the telencephalon, as opposed to in the diencephalon (**Fig. 3g–i**). Notably, the overwhelming majority of *Dbx1*-positive and *Dbx1*-derived cells accumulated in the region of the developing amygdala. Therefore, on the basis of these patterns of β-galactosidase expression in two sets of mice that mark *Dbx1*-expressing cells and their progeny, it appears that two spatially separated *Dbx1*-positive progenitor regions, the ventral pallium and POA, are probably the primary sources of the postnatal *Dbx1*-derived amygdala cells that we observed (**Fig. 2**).

To more closely examine the patterns of putative migration from these sources, we crossed $Dbx1^{+/CreERT2}$ mice with *R26R-YFP* reporter mice, which express yellow fluorescent protein (YFP) in the presence of Cre recombinase[20] (**Fig. 4**). In contrast with β-galactosidase, YFP is typically expressed in the entire cell, which allows for examination of migratory profiles. Tamoxifen treatment at E9.5 resulted in the appearance of recombined cells emanating from the POA, with leading processes being primarily oriented toward the basal telencephalon (**Fig. 4a–c**). Notably, only a few YFP-positive cells could be detected along the LCS at this age of tamoxifen delivery. In contrast, E10.5 tamoxifen treatment resulted in the generation of numerous YFP-positive cells along the LCS, as well as a continued putative migration from the region of the POA (**Fig. 4d–i**). To our surprise, many of the *Dbx1*-derived cells of the LCS did not express Pax6, a pallial marker that is typically expressed in many cells of the LCS[8]. The leading processes of many of POA-derived and LCS recombined cells were oriented toward the basal telencephalon, suggestive of active migration to the developing amygdala. Notably, the orientation of the leading processes of the *Dbx1*-derived POA population appeared to be different from that of *Dbx1*-derived cells along the LCS, indicating that these were two separate migratory populations (**Fig. 4d**,**e**).

Thus, our analysis of the patterns of β-galactosidase and YFP expression in a series of mice in which *Dbx1*-positive cells and their progeny were marked (**Figs. 3** and **4**) indicate that the postnatal *Dbx1*-derived cells in the amygdala (**Fig. 2**) primarily originated in the ventral pallium and POA. These analyses also revealed that *Dbx1*-derived cells of the POA were generated earlier in development than the *Dbx1*-derived cells of the ventral pallium. This also correlates with the 1-d difference in the timing of the generation of *Dbx1*-derived medial nuclei cells versus *Dbx1*-derived basolateral complex cells described above (**Fig. 2**).

POA-derived cells are highly migratory

Although our results suggested that *Dbx1*-derived cells of the POA migrate to the developing amygdala, we wanted to directly examine and

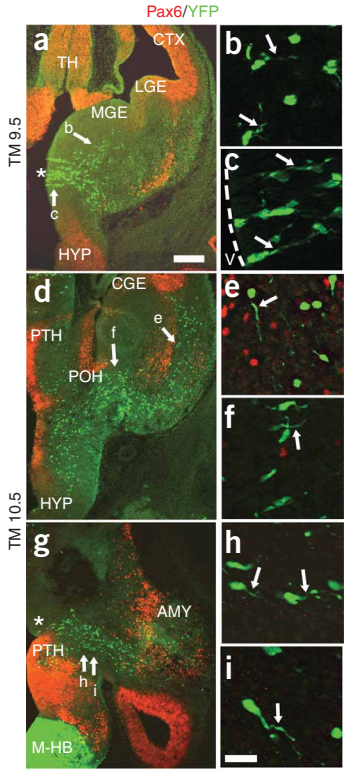

Figure 4 Distribution of YFP-positive recombined cells at embryonic stages. (**a**–**i**) Tamoxifen was administered to *Dbx1*$^{+/CreERT2}$;*R26R-YFP* embryos at E9.5 (**a**–**c**) or E10.5 (**d**–**i**) and analyzed at E12.5. E9.5 tamoxifen administration resulted in YFP-positive recombined cells (green) primarily in the POA (asterisk), with only a few YFP-positive recombined cells being observed along the LCS, as shown in a coronal section at low-power magnification (**a**). Higher-power magnification of areas highlighted by arrows in **a** shows leading processes of recombined cells (arrows, **b**,**c**). Numerous recombined cells were observed in the ventricular zone (VZ) of the POA (**c**, dotted line marks the edge of the tissue and the location of the lateral ventricle 'v'). As shown in a low-power coronal section (**d**), E10.5 tamoxifen administration (**d**,**g**) resulted in recombined cells along both the PAS migratory stream (arrow, **f**) and LCS (arrow, **e**). Higher-power magnification shows Pax6 (red) negative, recombined cells along the LCS with migratory profiles directed toward the basal telencephalon (arrow, **e**). Recombined PAS cells also showed migratory profiles directed toward the developing amygdala (arrow, **f**). The PAS migratory stream is most evident in horizontal sections (**g**, asterisk marks the POA), with higher-power magnification of YFP-positive cells also revealing recombined cells with leading processes oriented toward the developing amygdala (arrows, **h**,**i**). AMY, developing amygdala; M-HB, midbrain-hindbrain region; PTH, prethalamus; TH, thalamus. The scale bar in **a** represents 250 μm and also applies to panels **d** and **g**. The scale bar in **i** also applies to panels **b**, **c**, **e**, **f** and **h** and represents 20 μm.

compare their migratory capacity to that of the PSB and septum, the two other telencephalic domains of *Dbx1*-positive expression (**Fig. 1**). First, we dissected the POA, PSB and septum from E12.5 embryos and cultured them for 3 d *in vitro* (DIV) in matrigel, a permissive substrate for migration (**Supplementary Fig. 3** online). The majority (17 out of 21) of POA explants showed moderate to robust migration (**Supplementary Fig. 3**). This is in contrast to explants from the septum, from which either no or minimal migration was observed (**Supplementary Fig. 3**). Consistent with our previous studies[8], most (14 out of 16) PSB explants also showed robust migration (**Supplementary Fig. 3**).

Second, we carried out a series of 1,1′-dioctadecyl-3,3,3′,3′-tetramethylindocarbocyanine perchlorate (DiI)-labeling experiments in telencephalic slices from *Dbx1*$^{+/CreERT2}$;*R26R-YFP* embryos at E13.5 (**Fig. 5**). After 2 DIV, numerous DiI-positive cells from the POA and PSB migrated toward the region of the developing amygdala (**Fig. 5a**,**b**,**f**,**g**). Many DiI-positive cells from both the PSB and POA also expressed YFP (**Fig. 5c–e**,**h–m**), indicating that these migratory streams were comprised, at least in part, of *Dbx1*-derived cells. Notably, the PAS was also marked by expression of *Dlx2*$^{+/tauLacZ}$ and *Lhx2*, suggesting that this migratory route is comprised of a heterogeneously marked population of cells (**Fig. 5n–o**). Although their mode of migration remains unknown, *Dbx1*-derived cells of the POA also intermingled with radial glia, suggesting that these cells may migrate along radial glia (**Supplementary Fig. 4** online).

Fate of *Dbx1*-derived cells in the postnatal amygdala

On the basis of their location in the pallium and subpallium, respectively, we predicted that ventral pallial *Dbx1*-derived cells give rise to amygdala excitatory neurons and the POA *Dbx1*-derived cells give rise to amygdala inhibitory neurons. To test this, we examined whether *Dbx1*-derived cells from these locations express regional

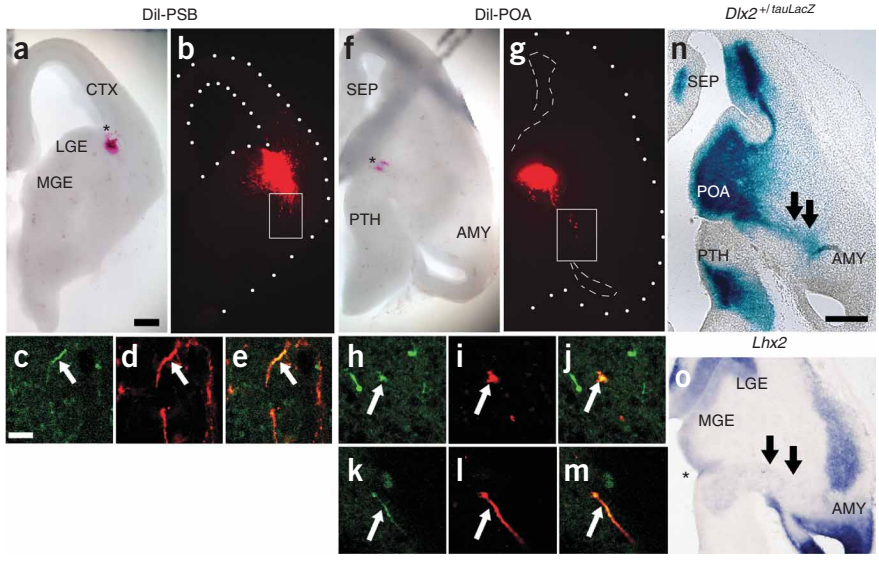

Figure 5 Migration from the PSB and POA. (**a**–**j**) DiI crystals (red) were placed in either the PSB in coronal slices (**a**,**b**, $n = 2$) or in the POA (**f**,**g**, $n = 4$) in horizontal slices at E13.5 in *Dbx1*$^{+/CreERT2}$;*R26R-YFP* embryos treated with tamoxifen at E10.5. After 2 DIV, DiI-labeled cells (red) from both the PSB and the POA migrated to the basal telencephalon (**b**,**g**). Boxed regions show that migratory streams from both the PSB (arrows, **c**–**e**) and POA (arrows, **h**–**j**) comprise *Dbx1*-derived cells, as revealed by coexpression of DiI (red) and YFP (green). (**k**–**m**) Cells coexpressing DiI and YFP are also shown from another brain slice (arrows). (**n**,**o**) β-galactosidase–stained horizontal sections from E12.5 *Dlx2*$^{+/tauLacZ}$ embryos (**n**) and *Lhx2* mRNA expression (**o**) also marked the PAS migratory route (double arrows, asterisk marks the POA in **o**). The scale bar in **a** also applies to panels **b**, **f** and **g**, and represents 250 μm. The scale bar in **c** also applies to panels **d**, **e** and **h**–**m**, and represents 50 μm. The scale bar in **n** also applies to panel **o** and represents 250 μm.

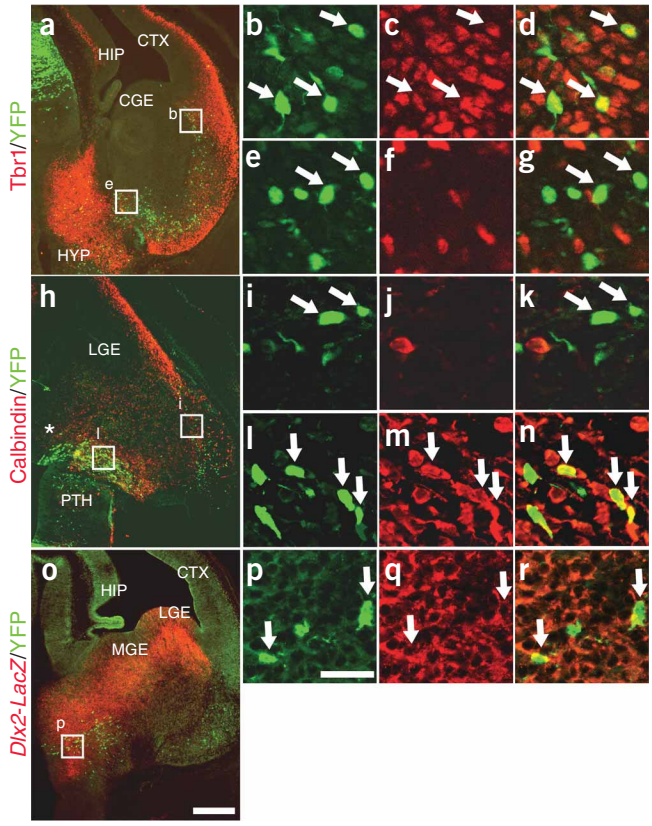

Figure 6 *Dbx1*-derived cells express regional cell fate markers during embryogenesis. (**a**–**r**) The expression of Tbr1 (**a**–**g**) and calbindin (**h**–**n**) in *Dbx1*$^{+/CreERT2}$*;R26R-YFP* embryos and Dlx2 (**o**–**r**) in *Dbx1*$^{+/CreERT2}$*;R26R-YFP;Dlx2*^{tauLacZ} embryos at E12.5 in which tamoxifen was administered at E10.5. As shown in a coronal section (**a**), expression of Tbr1 (red) was detected in 90.2% (46 out of 51) of YFP-positive recombined cells (green) along the LCS (boxed region **b** and arrows in **b**–**d** show double labeled cells). In contrast, Tbr1 was not detected in any (0 out of 33) YFP-positive recombined cells along the PAS (boxed region **e** and arrows in **e**–**g** show lack of double labeling). As shown in a horizontal section (**h**), no (0 out of 88) YFP-positive recombined cells (green) of the LCS coexpressed calbindin (red) (boxed region **i** and arrows in **i**–**k** show lack of double labeling). However, 41.4% (46 out of 111) of YFP-positive recombined cells of the PAS (green) coexpressed calbindin (red) (boxed region **i** and arrows in **l**–**n** show double-labeled cells). As shown in a coronal section (**o**), 80.8% (21 out of 26) of YFP-positive recombined cells of the PAS (green) also coexpressed Dlx2 (red) (boxed region **p** and arrows in **p**–**r** show double-labeled cells). Asterisks in **h** and **o** mark the POA. The scale bar in **o** also applies to panels **a** and **h** and represents 250 μm. The scale bar in **p** also applies to panels **b**–**g**, **i**–**n** and **p**–**r**, and represents 20 μm.

neuronal subtype markers. In these experiments, sections from E12.5 *Dbx1*$^{+/CreERT2}$*;R26R-YFP* embryos in which tamoxifen was administered at E10.5 were double immunolabeled with a variety of well-characterized cell-specific markers, including Tbr1, a marker of developing and mature telencephalic excitatory neurons[21], and calbindin and Dlx2, broad markers of developing inhibitory neurons[22,23] (**Fig. 6**). Consistent with their pallial origin, numerous *Dbx1*-derived cells of the LCS expressed Tbr1 (90.2%), but did not express calbindin (**Fig. 6a–n**). In contrast, *Dbx1*-derived cells of the PAS did not express Tbr1 (**Fig. 6a–g**), but instead many expressed the subpallial markers calbindin (41.4%) or Dlx2 (80.8%) (**Fig. 6h–r**). Thus, it appears that *Dbx1*-derived cells of the ventral pallium generate amygdala excitatory neurons and *Dbx1*-derived cells of the PAS differentiate into inhibitory neurons.

We next examined the postnatal cellular fate of *Dbx1*-derived cells in the amygdala (**Fig. 7**). Tbr1 was used to mark excitatory cells and, from the results of previous studies on amygdala neuronal cell diversity, nNOS, calretinin and calbindin were used to mark mature inhibitory neurons[24,25]. Our analyses revealed that all of the *Dbx1*-derived cells in the basolateral complex and most (95.3%) of the cells in the cortical

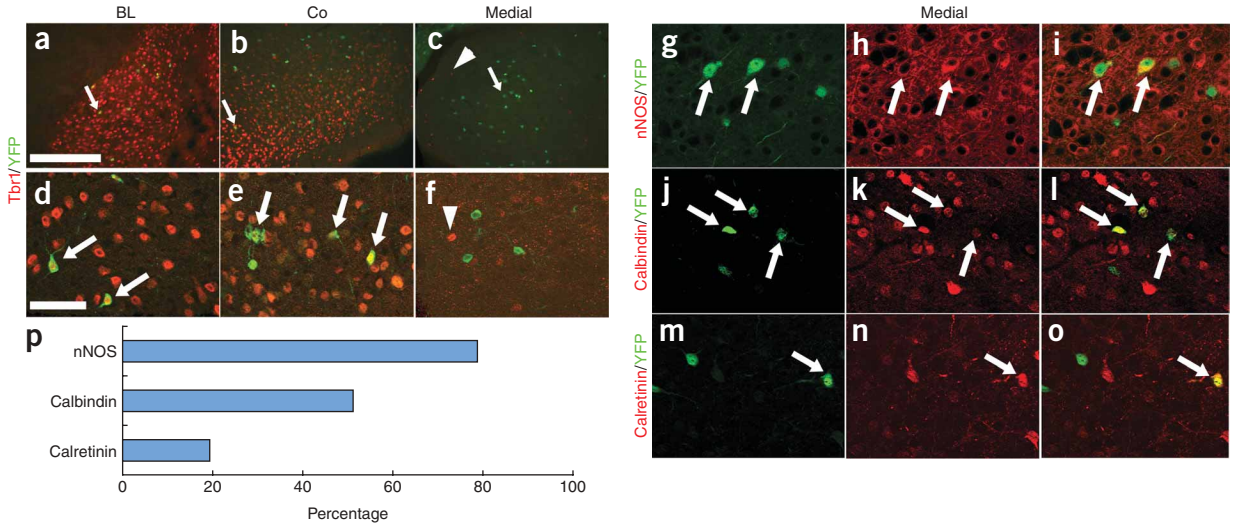

Figure 7 *Dbx1*-positive progenitors generate amygdala excitatory and inhibitory neurons. (**a**–**f**) We examined the cellular phenotype of recombined cells in the amygdala at P21 in *Dbx1*$^{+/CreERT2}$*;R26R-YFP* mice that were administered tamoxifen at E10.5. All (32 out of 32) YFP-positive recombined cells (green) in the basolateral complex (**a**,**d**) and 95.3% (41/43) of recombined cells in the cortical nucleus (**b**,**e**) were positive for Tbr1 (red), as shown at low- and high-power magnification (arrows show double-labeled cells). In contrast, no (0 out of 41) YFP-positive recombined cells (green, arrow) in the medial nucleus expressed Tbr1 (arrowhead) (**c**,**f**). (**g**–**o**) Higher-power magnification of the medial nucleus revealed YFP-positive recombined cells coexpressing nNOS (arrows, **g**–**i**), calbindin (arrows, **j**–**l**) or calretinin (arrows, **m**–**o**). (**p**) The percentages of YFP-positive cells coexpressing each inhibitory marker in the medial nucleus are shown (78.6% (114 out of 145) of recombined YFP-positive cells in the medial nucleus were positive for nNOS, 50.8% (30 out of 59) were positive for calbindin and 19.1% (18 out of 94) were positive for calretinin). The scale bar in **a** applies to panels **a**–**c** and represents 250 μm. The scale bar in **d** applies to panels **d**–**o** and represents 20 μm.

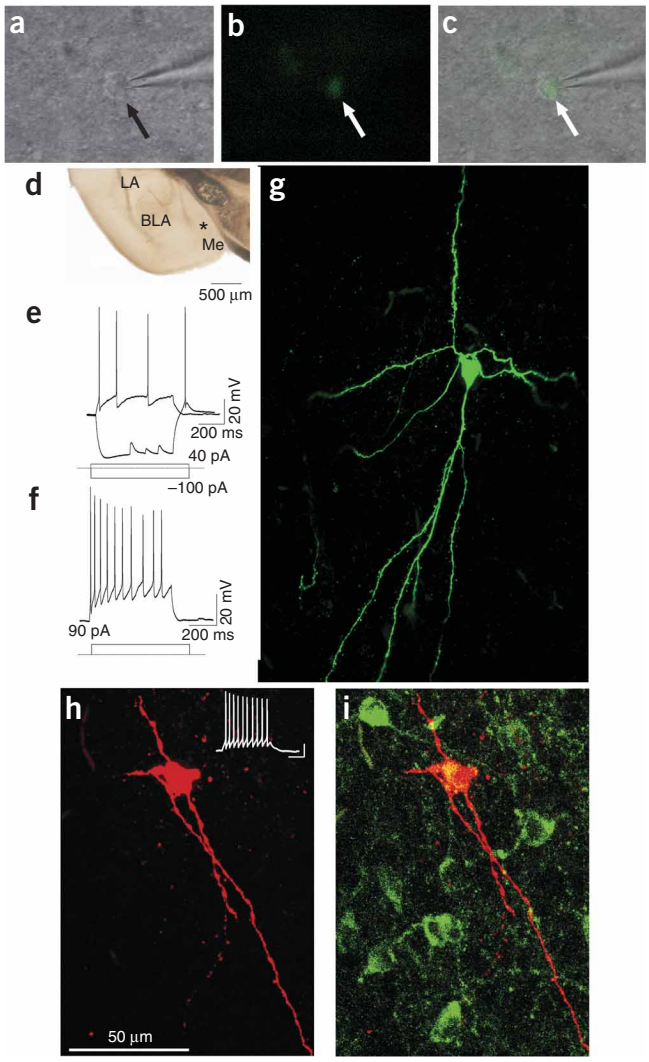

Figure 8 Electrophysiological properties of *Dbx1*-derived medial amygdala neurons. (**a**–**c**) Differential interference contrast (**a**), fluorescent (**b**) and overlay (**c**) images of a typical YFP-positive recombined medial amygdala neuron (arrows) with attached recording electrode. (**d**) Live coronal slice indicating the region of physiological recordings (asterisk). (**e**,**f**) Firing patterns of a typical medial amygdala YFP-positive recombined cell at threshold and subthreshold (**e**) and suprathreshold (**f**) firing. The injected level of current for each trace is indicted below. (**g**) Confocal image of the biocytin-filled cell represented in **d** and **e** following physiological characterization. Note the fusiform-like dendritic arborization and the presence of sparsely spiny dendrites. (**h**) Confocal image of biocytin-filled cell conjugated to Texas red following whole-cell patch-clamp recording. The current-clamp trace of this cell is located in the upper right corner (scale bars represent 200 ms (horizontal) and 20 mV (vertical)). (**i**) Fluorescent immunostaining for nNOS (green) revealed that this cell was also nNOS positive (yellow).

nucleus were Tbr1 positive (**Fig. 7a**,**b**,**d**,**e**). In contrast, none of the recombined cells in the medial nucleus, a region that is only sparsely populated by excitatory neurons, were Tbr1 positive (**Fig. 7c**,**f**). Instead, most (78.6%) of the recombined cells of the medial amygdala expressed nNOS, a marker of medial nuclei projection neurons[26] (**Fig. 7g–i**,**p**). In addition, 50.8% of YFP-positive cells in the medial nucleus expressed calbindin and 19.1% expressed calretinin (**Fig. 7j–p**), consistent with an inhibitory neuronal fate. Thus, *Dbx1*-derived cells give rise to both excitatory and inhibitory cell diversity in the postnatal amygdala.

Collectively, these results indicate that the *Dbx1*-derived cells of the ventral pallium and POA are major differential sources of this excitatory and inhibitory cell diversity in the basolateral complex/cortical nuclei and medial nuclei, respectively, in the postnatal amygdala. The evidence in support of this is threefold. First, the *Dbx1*-derived cells of the POA were generated 1 d earlier than those of the ventral pallium (**Fig. 4**). This correlates with the 1 d earlier generation of *Dbx1*-derived cells in the mature medial nucleus as compared with the basolateral complex (**Fig. 2**). Second, the leading processes of ventral pallium and POA *Dbx1*-derived cells were oriented toward the developing amygdala, indicating that these two regions are separate sources of migrating cells (**Fig. 4**). Finally, during their migration to the developing amygdala, ventral pallium and POA *Dbx1*-derived cells expressed excitatory and inhibitory neuronal markers, respectively (**Fig. 6**).

Physiological analysis of *Dbx1*-derived medial nuclei cells

In addition to expressing unique combinations of immunomarkers, subtypes of telencephalic inhibitory neurons also have distinct electrophysiological signatures[27]. To determine whether *Dbx1*-derived neurons possess functional features of inhibitory neurons, we carried out whole-cell patch-clamp recordings of recombined YFP-positive cells in the medial nucleus from *Dbx1*$^{+/CreERT2}$;*R26R-YFP* mice at P17–27 (**Fig. 8** and **Supplementary Table 1** online). YFP-positive neurons in the medial amygdala were identified under fluorescent and infrared differential interference contrast video microscopy (**Fig. 8a–c**). The average *Dbx1*-derived neuron had a membrane potential of –58.21 ± 1.1 mV ($n = 35$) with an input resistance at 491.34 ± 26.7 MΩ ($n = 35$). Action-potential discharge patterns were obtained by injecting current pulses in current-clamp mode and monitoring discharge responses. A notable feature of *Dbx1*-derived neurons is the lack of diversity in action-potential firing patterns, as all ($n = 35$) recorded cells showed accommodating firing patterns (accommodation ratio = 0.568 ± 0.029) at threshold and all had sharp rising after hyperpolarizing potentials (**Fig. 8d–f**).

In addition, *Dbx1*-derived neurons shared some biochemical and physiological similarities with inhibitory neurons in other brain regions. For example, although there were differences in many characteristics, the firing pattern was similar to the recently identified nNOS-positive 'Ivy cells' of the hippocampus[28] and the calretinin-positive classic-accommodating 'Martinotti cells' of the cerebral cortex[29]. In addition, at hyperpolarizing current pulses in the –100-pA range, *Dbx1*-derived neurons revealed a small sag (4.1 ± 0.55 mV $n = 27$) that was indicative of an I_h current and, at the conclusion of the 600-ms hyperpolarizing pulse, caused a rebound burst that was indicative of low-threshold calcium currents in the inhibitory low threshold–spiking cells of the cerebral cortex[30–32]. Current pulses at more negative levels were deleterious to the cells and resulted in rapid depolarization in membrane potential. As revealed by biocytin filling, *Dbx1*-derived cells possessed large, sparsely spiny proximal dendrites with numerous long, typically bipolar–oriented projections (**Fig. 8g–i** and **Supplementary Fig. 5** online). This morphology is similar to recently characterized medial amygdala neurons, some of which show inhibitory characteristics[33]. Therefore, a combination of immunomarker, electrophysiological and morphological analyses (**Figs. 7** and **8**) indicate that *Dbx1*-derived neurons, although sharing similarities with a variety of classic inhibitory features outside of the amygdala, appear to be a distinct subclass of neurons.

DISCUSSION

By a combination of *in vivo* and *in vitro* approaches, including genetic fate mapping, cell migration assays and electrophysiology, we examined

the link between the embryonic origin of progenitor cells and their fate in the mature amygdala. Our primary finding is the identification of a neural progenitor pool that is specifically dedicated to the generation of a single subtype of inhibitory neuron in the mature medial amygdala nucleus, a major inhibitory output nucleus of the amygdala. Our results reveal that this population, which is marked by the expression of the homeodomain-encoding gene *Dbx1*, migrates along a newly identified migratory stream, the PAS, which arises from the POA of the subpallial telencephalon, a region that has not been previously recognized, to the best of our knowledge, as a source of migratory cells. Moreover, our analyses indicate that the ventral pallial *Dbx1*-positive population is a source of excitatory neurons in the basolateral complex and cortical nuclei, the two major excitatory nuclei of the amygdala (**Supplementary Fig. 6** online). These findings also provide strong support for an emerging model in which aspects of the program for the development of the amygdala are distinct from that of other telencephalic structures such as the cerebral cortex.

Differential sources of amygdala inhibitory and excitatory neurons

The embryonic subpallium is the origin of most, if not all, inhibitory neuronal cell populations in the cerebral cortex and striatum[27,34,35]. It also appears that the vast inhibitory interneuronal diversity that is characteristic of the telencephalon is derived from spatially distinct progenitor pools in the subpallial ganglionic eminences, most prominently the medial and caudal ganglionic eminences (MGE and CGE, respectively). Emerging evidence also suggests that the genetic mechanisms for the establishment of inhibitory neuronal cellular diversity in the telencephalon are markedly similar to those in the spinal cord, in which the combinatorial expression of specific transcription factor genes (typically of the homeodomain and bHLH classes) intrinsically instructs spatially separate progenitor populations to give rise to mature neurons with differential functional fates[27,36]. Consistent with this idea of 'combinatorial genetic codes', recent studies have revealed that the subpallium can be subdivided into at least 18 distinct progenitor zones[37]. One of these unique regions is the POA, which is distinguished in part by its focal expression of *Dbx1*. Using of a Cre-based fate-mapping strategy combined with *in vitro* migratory assays, we identified a POA migratory stream, termed the PAS, that is comprised, at least in large part, of *Dbx1*-derived progenitors. As the POA and PAS was also combinatorially marked by a number of other transcription factors, most notably *Nkx6.2*, *Lhx2* and *Dlx1/2* (data shown in **Fig. 5**)[37], it is probable that, similar to the LCS migratory route from the PSB, the PAS may be comprised of a diverse set of progenitor cells.

The primary function of the medial amygdala is to process sensory information from the olfactory bulb and relay this information to the hypothalamus, a brain region involved in hormonal regulation. As such, the medial amygdala has reciprocal connections with multiple hypothalamic nuclei, which in turn project to numerous regions of the brainstem. These pathways are involved in the regulation of social, feeding and reproductive behaviors[3,38]. Along with the central nucleus, the medial amygdala comprises the major inhibitory output of the amygdala. The predominant neuronal subtype of the medial amygdala is the inhibitory projection neurons. On the basis of their electrophysiological properties, cellular morphology and expression of nNOS, the *Dbx1*-derived medial amygdala neurons resemble a previously characterized population of inhibitory projection neurons of the medial nucleus[26,33]. Although their function remains unknown, these nNOS-positive neurons project to the paraventricular nucleus of the hypothalamus and may therefore be involved in the modulation of hormone release and autonomic responses. Thus, in addition to identification of a *Dbx1*-derived POA-amygdala migratory stream, our results indicate that these cells generate a specific subtype of inhibitory neurons in the medial amygdala, and therefore uncover a previously unknown relationship between gene expression, developmental origin and electrophysiological fate in the amygdala.

The PSB comprises progenitors from the ventral pallium and dLGE aspects of the developing telencephalon. These progenitors migrate to the basal telencephalic limbic system via the LCS[8,39]. A series of studies has revealed that ventral pallium and dLGE progenitors express a combination of markers that define this region as distinct from other telencephalic progenitor domains[9–11,40,41]. On the basis of their expression of pallial markers, such as *Pax6*, the ventral pallium population is predicted to give rise to excitatory neurons. In contrast, dLGE progenitors, which express subpallial markers such as *Gsx2* and *Dlx1/2*, may generate subtypes of inhibitory neurons of the amygdala. To the best of our knowledge, however, a direct link between gene expression domains of the PSB and neuronal cell fate in the amygdala has not yet been demonstrated. Our data indicate that *Dbx1*-positive progenitors derived from the ventral pallium are a source of excitatory neurons of the basolateral complex and cortical amygdala nuclei, major excitatory outputs of the amygdala. During their migration along the LCS, a subpopulation of these basally migrating *Dbx1*-derived cells expressed Tbr1, a marker of excitatory neurons, but did not express Pax6. As Pax6 expression marks a large number of LCS cells[8,12,13,41,42], this result was somewhat surprising and indicates that the ventral pallium generates a heterogeneous pool of progenitors destined for the amygdala. In addition to the ventral pallium as a source of excitatory cells of the amygdala, fate-mapping studies of *Emx1*-derived cells, whose expression marks more dorsally located progenitors in the lateral pallium, have revealed that *Emx1*-derived cells are also a presumptive source of amygdala excitatory neurons[43,44]. Whether these progenitor populations, which are differentially marked by *Dbx1*, *Pax6* and/or *Emx1*, give rise to distinct functional and or spatially located excitatory neurons in the mature amygdala remains to be explored.

Comparison of amygdala development to other brain regions

A number of recent studies have revealed that there are notable similarities between the development of the amygdala and other major telencephalic structures, such as the cerebral cortex and striatum. The main commonality is a sharing of progenitor populations for the generation of neuronal diversity. For example, *in utero* cell transplantation fate-mapping and gene-expression studies have revealed that the ventral telencephalic MGE and CGE are sources of inhibitory interneuronal cell diversity for the amygdala, cerebral cortex and striatum[45,46]. In addition, recent genetic fate-mapping studies have revealed that subpallial progenitors expressing *Nkx2.1* generate parvalbumin interneuronal subtypes in both the amygdala and cerebral cortex[47]. Moreover, the lateral olfactory tract nucleus of the amygdala appears to share a common developmental origin with the cerebral cortex[48].

However, our finding of a point-to-point correlation between the *Dbx1*-derived POA source and the medial nucleus of the amygdala suggests a putative additional mechanism for the generation of neuronal cell diversity in the amygdala in which there also exists progenitor pools that are set aside exclusively for the limbic system. This is consistent with and predicted by previous molecular anatomical studies, which have identified combinations of genes whose expression marks both embryonic progenitor domains and individual emerging amygdala nuclei, including the medial and central nuclei, suggesting a developmental relationship between the two[9,49]. A major prediction of these gene-expression studies is that progenitor pools that express unique combinations of genes will generate distinct functional cell types. As revealed by our studies, at least in the case of the *Dbx1*-derived

POA population, this progenitor pool gives rise almost exclusively to a single functional subtype of inhibitory neurons of the medial amygdala. Although possessing some characteristics that are shared with other telencephalic inhibitory cell types, a combination of criteria including neuronal subtype marker expression, cell morphology and electrophysiological properties indicates that the POA *Dbx1*-derived neurons of the medial amygdala appear to be distinct from other telencephalic inhibitory cell types. Therefore, our data, in conjunction with previous studies, suggest a model in which there are both overlapping and distinct mechanisms for amygdala development in comparison with other telencephalic structures. Thus, for the generation of cell types that are found in other brain regions (such as parvalbumin interneurons which are generated in the MGE), there are shared progenitor pools. In contrast, the generation of cell types that may be exclusive to the amygdala, such as the medial amygdala *Dbx1*-derived inhibitory neurons, appears to require dedicated progenitor pools.

In summary, our data provide new and important insight into the developmental mechanisms underlying the generation of neuronal diversity in the amygdala, a brain structure that is essential for major aspects of complex mammalian behavior. First, we identified a previously unknown major migratory stream (the PAS) in the developing brain that is comprised of *Dbx1*-positive progenitors that are derived from the POA. Because this population generates a specific cell type in a distinct functional nucleus of the amygdala, we found a direct correlation between an embryonic progenitor population and a functional neuronal cell type in the mature telencephalon. Second, our data reveal major differences between the mechanisms of the development of the amygdala and the cerebral cortex and thus support a revised model of brain development. In addition, as altered function of the amygdala is a hallmark characteristic of neurodevelopmental disorders such as autism and autism spectrum disorders, our findings may provide a framework for a deeper understanding of the etiology of these disorders.

METHODS

Generation of CreER^{T2} knock-in mice. All procedures involving the use of animals were carried out in accordance with approved procedures established by the Children's National Medical Center and Georgetown University Animal Care and Use Committees. The *Dbx1*$^{+/CreERT2}$ targeting construct was generated by targeting an IRES-CreER^{T2}-FRT-NEO-FRT cassette into the *Bam*HI site at the 3′ UTR of the *Dbx1* locus (obtained from mouse 129sv strain RCPI 21 PAC library, Invitrogen), the same site that was previously used to knock *cre* into the *Dbx1* locus[11]. Correctly targeted R1 embryonic stem cells were injected into C57BL/6 blastulas and chimeric offspring were crossed to C57BL/6 mice. The neomycin resistance gene was removed by crossing heterozygous *Dbx1*$^{+/CreERT2}$ mice to FLPeR (flipper) mice (Jackson Labs).

Reporter mouse lines and tamoxifen delivery. *R26R-LacZ* and *R26R-YFP* reporter mice were obtained from Jackson Labs. Tamoxifen (Sigma, T5648) was dissolved at a concentration of 20 mg ml^{-1} in corn oil (Sigma C8267) and administered by oral gavage to pregnant dams at a concentration of 4–8 mg per 40 g of mouse body weight.

Immunohistochemistry and β-galactosidase staining. Embryos were fixed with 4% paraformaldehyde (wt/vol) for 2 h at 4 °C, dehydrated in 30% sucrose (wt/vol), embedded in OCT embedding compound and sectioned at 30 μm. For detection of β-galactosidase expression in *Dbx1*$^{+/LacZ}$ knock-in, *Dbx1*$^{+/CreERT2}$;*R26R-LacZ* and *Dlx2*$^{+/tauLacZ}$ embryos, sections were incubated in the X-gal staining solution overnight at 37 °C. For detection of *Dlx2* expression, *Dbx1*$^{+/CreERT2}$;*R26R-YFP* mice were crossed to previously generated *Dlx2*$^{+/tauLacZ}$ mice, in which β-galactosidase expression faithfully recapitulates *Dlx2* expression[50]. For immunohistochemistry, sections were incubated with the primary antibody at 4 °C overnight, washed and incubated with the corresponding fluorescent secondary antibodies. For primary antibodies, we used goat antibody to β-galactosidase (1:400; Biogen), rabbit antibody to Tbr1 (1:2,000; kind gift from R. Hevner, University of Washington), rabbit antibody to Pax6 (1:500; Covance Research Products), rabbit antibody to nNOS (1:1,000; Sigma), goat antibody to GFP (to detect YFP expression, 1:500; Novus), rabbit antibody to calbindin (1:500; Calbiochem), rabbit antibody to calretinin (1:1,000; Millipore) and mouse antibody to RC2 (1:5; Developmental Hybridoma Studies Bank).

***In situ* hybridization.** Embryos were processed and sectioned as described above. Sections were refixed with 4% paraformaldehyde and subsequently treated with proteinase K, refixed with 4% paraformaldehyde, treated with triethanolamine containing acetic anhydride and then hybridized with digoxigenin-UTP–labeled RNA probes overnight. The next day, the probes were washed with 50% formamide, 2× SSC at 65 °C, treated with 20 mg RNase and washed in 50% formamide in 2× SSC at 65 °C. Signals were detected with an antibody to digoxigenin (Roche) and BM purple (Roche). The probes used in this study were *Dbx1* (**Fig. 1**)[9], *Foxg1* (ref. 14), *Lhx2* (ref. 37) and *cre* recombinase (5′ coding region was subcloned into pBlusescript and RNA probe was generated from NcoI digested plasmid using T3 RNA polymerase). For analysis of *Dbx1* expression in *Dbx1*$^{+/CreERT2}$ embryos (**Supplementary Fig. 1**), a PCR-amplified fragment of the 5′ coding region was subcloned into pBluescript and an RNA probe was generated from *Bam*HI-digested plasmid using T7 RNA polymerase.

Migration assays. For matrigel assays, tissue was dissected from E12.5 embryos using Lumsden Bioscissors. The explants were placed in matrigel (BD Biosciences) mixed with L-15 media and cultured in Neurobasal medium (Invitrogen), supplemented with penicillin/streptomycin (1:100; Invitrogen), B27 supplement (1:50; Invitrogen) and glutamine (1:100; Invitrogen). After 3 DIV, explants were fixed in 4% paraformaldehyde for 30 min, rinsed briefly in PBS, covered with 50% glycerol and photographed. For DiI migration assays, 300-μm horizontal or coronal slices were cut from E13.5 embryos with a vibratome, and DiI crystals were placed in the POA or ventral pallium and cultured in Neurobasal medium (Invitrogen), supplemented with penicillin/streptomycin (1:100; Invitrogen), B27 supplement (1:50; Invitrogen) and glutamine (1:100; Invitrogen). After taking low-power pictures of both light field and fluorescence, specimens were fixed in 4% paraformaldehyde for 2 h, re-sectioned on a vibratome at 100 μm and processed for immunofluorescence.

Electrophysiology and biocytin. We killed the mice and immediately immersed their brains in ice-cold oxygenated (95% O_2/5% CO_2) sucrose solution (234 mM sucrose, 11 mM glucose, 24 mM $NaHCO_3$, 2.5 mM KCl, 1.25 mM $NaH_2PO_4H_2O$, 10 mM $MgSO_4$ and 0.5 mM $CaCl_2$). Coronal slices were cut on a vibratome (Leica) at 250 μm and placed in preheated (32 °C), oxygen-equilibrated artificial cerebral spinal fluid for 1 h. Slices were then placed in a recording chamber and visualized with a fixed-staged, upright microscope (Nikon, E600 FN) equipped with infrared illumination, Nomarski optics, an infrared-sensitive video camera (COHU) and fluorescent lamp (Nikon) with a 450–490λ filter. Intracellular pipettes were pulled with a Flaming/Brown Micropipette Puller (Sutter Instruments) to a resistance of 3–5 MΩ when filled with a solution containing 130 mM potassium gluconate, 10 mM KCl, 10 mM HEPES, 10 mM EGTA and 2 mM $MgCl_2$. YFP-positive fluorescent cells were recorded at 21–23 °C with continuous perfusion of artificial cerebral spinal fluid in current-clamp mode (Multiclamp 700A, DigiDATA, Axon). After recording membrane potential and input resistance values, cells were categorized on the basis of their response to depolarizing and hyperpolarizing current pulses. The response properties were analyzed off-line using pClamp software (Axon) and graphing software (Origin).

In some cases, post recording, biocytin (1%) was injected with depolarizing current pulses (1 nA). Pictures were taken with an image-capturing (Scion) system to relocate the cells post processing. A subset of tissue with biocytin-filled cells was also processed for nNOS immunohistochemistry. In these cases, the slices were removed from the recording chamber, fixed overnight in 4% paraformaldehyde and processed for immunohistochemistry.

Microscopy. Light-microscopic photographs were taken using an Olympus BX51 microscope and an Olympus CKX41 inverted microscope. Fluorescent photographs were taken using an Olympus BX61 (for low-power fluorescence

and low-power DiI images), a Zeiss Apotome (for high-power fluorescence), a Zeiss LSM510 confocal microscope (for high-power DiI/YFP double fluorescence) or an Olympus Fluoview Laser Scanning Confocal Microscope (for biocytin-filled cells). Any brightness and contrast adjustments were done equally across pictures using Adobe Photoshop.

Note: Supplementary information is available on the Nature Neuroscience website.

ACKNOWLEDGMENTS

The authors would like to thank members of the Corbin, Haydar and Zohn laboratories for input during various stages of this project, with a special acknowledgment to J.L. Olmos-Serrano for his expert insight and advice on amygdala anatomy and development. We also gratefully acknowledge T. Haydar, J.L. Olmos-Serrano, I. Zohn and V. Gallo for critical reading of the manuscript. We thank R. Hevner for the Tbr1 antibody (University of Washington), S. Aizawa for the *Foxg1* and *Lhx2* probes (RIKEN) and M. Matise for the *Dbx1* probe (University of Medicine and Dentistry New Jersey/Robert Wood Johnson Medical School). The RC2 monoclonal antibody was obtained from the Developmental Studies Hybridoma Bank developed under the auspices of the US National Institute of Child Health and Human Development and maintained by the University of Iowa. We also thank the Children's National Medical Center and Georgetown University Transgenic Cores for the generation of mice. This work was supported by grants from the US National Institutes of Health (J.G.C. and M.M.H.). The Children's National Medical Center microscope core facility is supported by an US National Institutes of Health Intellectual and Developmental Disabilities Research Center grant.

AUTHOR CONTRIBUTIONS

T.H. generated the *Dbx1*$^{+/CreERT2}$ knock-in animals and carried out the fate mapping, slice culture assays, immunohistochemistry and *in situ* hybridization analysis. G.M.L. provided timed crossed *Dbx1*$^{+/LacZ}$ embryos and input on the analysis. L.A.C. provided technical assistance for the slice culture migration assays and analysis. P.L. and M.M.H. obtained and analyzed the electrophysiological and biocytin data. J.G.C. carried out the matrigel experiments. The study was conceived and planned by T.H. and J.G.C. The majority of the manuscript was written by T.H. and J.G.C. with the electrophysiology part being written by M.M.H.

Published online at http://www.nature.com/natureneuroscience/
Reprints and permissions information is available online at http://npg.nature.com/reprintsandpermissions/

1. Alheid, G.F. Extended amygdala and basal forebrain. *Ann. NY Acad. Sci.* **985**, 185–205 (2003).
2. Sah, P., Faber, E.S., Lopez De Armentia, M. & Power, J. The amygdaloid complex: anatomy and physiology. *Physiol. Rev.* **83**, 803–834 (2003).
3. Swanson, L.W. & Petrovich, G.D. What is the amygdala? *Trends Neurosci.* **21**, 323–331 (1998).
4. Amaral, D.G., Bauman, M.D. & Schumann, C.M. The amygdala and autism: implications from nonhuman primate studies. *Genes Brain Behav.* **2**, 295–302 (2003).
5. Baron-Cohen, S. *et al.* The amygdala theory of autism. *Neurosci. Biobehav. Rev.* **24**, 355–364 (2000).
6. Rauch, S.L., Shin, L.M. & Phelps, E.A. Neurocircuitry models of posttraumatic stress disorder and extinction: human neuroimaging research–past, present, and future. *Biol. Psychiatry* **60**, 376–382 (2006).
7. Bai, J. *et al.* The role of DCX and LIS1 in migration through the lateral cortical stream of developing forebrain. *Dev. Neurosci.* **30**, 144–156 (2008).
8. Carney, R.S. *et al.* Cell migration along the lateral cortical stream to the developing basal telencephalic limbic system. *J. Neurosci.* **26**, 11562–11574 (2006).
9. Medina, L. *et al.* Expression of Dbx1, Neurogenin 2, Semaphorin 5A, Cadherin 8, and Emx1 distinguish ventral and lateral pallial histogenetic divisions in the developing mouse claustroamygdaloid complex. *J. Comp. Neurol.* **474**, 504–523 (2004).
10. Stenman, J., Toresson, H. & Campbell, K. Identification of two distinct progenitor populations in the lateral ganglionic eminence: implications for striatal and olfactory bulb neurogenesis. *J. Neurosci.* **23**, 167–174 (2003).
11. Bielle, F. *et al.* Multiple origins of Cajal-Retzius cells at the borders of the developing pallium. *Nat. Neurosci.* **8**, 1002–1012 (2005).
12. Yun, K., Potter, S. & Rubenstein, J.L. Gsh2 and Pax6 play complementary roles in dorsoventral patterning of the mammalian telencephalon. *Development* **128**, 193–205 (2001).
13. Carney, R.S.E., Cocas, L.A., Hirata, T., Mansfield, K. & Corbin, J.G. Differential regulation of telencephalic pallial–subpallial boundary patterning by *Pax6* and *Gsh2*. *Cereb. Cortex* published online, doi:10.1093/cercor/bhn123 (12 August 2008).
14. Tao, W. & Lai, E. Telencephalon-restricted expression of BF-1, a new member of the HNF-3/fork head gene family, in the developing rat brain. *Neuron* **8**, 957–966 (1992).
15. Branda, C.S. & Dymecki, S.M. Talking about a revolution: the impact of site-specific recombinases on genetic analyses in mice. *Dev. Cell* **6**, 7–28 (2004).
16. Joyner, A.L. & Zervas, M. Genetic inducible fate mapping in mouse: establishing genetic lineages and defining genetic neuroanatomy in the nervous system. *Dev. Dyn.* **235**, 2376–2385 (2006).
17. Soriano, P. Generalized lacZ expression with the ROSA26 Cre reporter strain. *Nat. Genet.* **21**, 70–71 (1999).
18. Danielian, P.S., Muccino, D., Rowitch, D.H., Michael, S.K. & McMahon, A.P. Modification of gene activity in mouse embryos *in utero* by a tamoxifen-inducible form of Cre recombinase. *Curr. Biol.* **8**, 1323–1326 (1998).
19. Pierani, A. *et al.* Control of interneuron fate in the developing spinal cord by the progenitor homeodomain protein Dbx1. *Neuron* **29**, 367–384 (2001).
20. Srinivas, S. *et al.* Cre reporter strains produced by targeted insertion of EYFP and ECFP into the ROSA26 locus. *BMC Dev. Biol.* **1**, 4 (2001).
21. Hevner, R.F. *et al.* Tbr1 regulates differentiation of the preplate and layer 6. *Neuron* **29**, 353–366 (2001).
22. Porteus, M.H., Bulfone, A., Ciaranello, R.D. & Rubenstein, J.L. Isolation and characterization of a novel cDNA clone encoding a homeodomain that is developmentally regulated in the ventral forebrain. *Neuron* **7**, 221–229 (1991).
23. del Rio, M.R. & DeFelipe, J. Colocalization of calbindin D-28k, calretinin and GABA immunoreactivities in neurons of the human temporal cortex. *J. Comp. Neurol.* **369**, 472–482 (1996).
24. McDonald, A.J. & Mascagni, F. Colocalization of calcium-binding proteins and GABA in neurons of the rat basolateral amygdala. *Neuroscience* **105**, 681–693 (2001).
25. Olmos, J.L., Real, M.A., Medina, L., Guirado, S. & Davila, J.C. Distribution of nitric oxide–producing neurons in the developing and adult mouse amygdalar basolateral complex. *Brain Res. Bull.* **66**, 465–469 (2005).
26. Tanaka, M. *et al.* Nitrergic neurons in the medial amygdala project to the hypothalamic paraventricular nucleus of the rat. *Brain Res.* **777**, 13–21 (1997).
27. Wonders, C.P. & Anderson, S.A. The origin and specification of cortical interneurons. *Nat. Rev. Neurosci.* **7**, 687–696 (2006).
28. Fuentealba, P. *et al.* Ivy cells: a population of nitric oxide–producing, slow-spiking GABAergic neurons and their involvement in hippocampal network activity. *Neuron* **57**, 917–929 (2008).
29. Wang, Y. *et al.* Anatomical, physiological and molecular properties of Martinotti cells in the somatosensory cortex of the juvenile rat. *J. Physiol. (Lond.)* **561**, 65–90 (2004).
30. Beierlein, M., Gibson, J.R. & Connors, B.W. Two dynamically distinct inhibitory networks in layer 4 of the neocortex. *J. Neurophysiol.* **90**, 2987–3000 (2003).
31. Bacci, A., Rudolph, U., Huguenard, J.R. & Prince, D.A. Major differences in inhibitory synaptic transmission onto two neocortical interneuron subclasses. *J. Neurosci.* **23**, 9664–9674 (2003).
32. Bacci, A., Huguenard, J.R. & Prince, D.A. Long-lasting self-inhibition of neocortical interneurons mediated by endocannabinoids. *Nature* **431**, 312–316 (2004).
33. Bian, X., Yanagawa, Y., Chen, W.R. & Luo, M. Cortical-like functional organization of the pheromone-processing circuits in the medial amygdala. *J. Neurophysiol.* **99**, 77–86 (2008).
34. Corbin, J.G., Nery, S. & Fishell, G. Telencephalic cells take a tangent: nonradial migration in the mammalian forebrain. *Nat. Neurosci.* **4** Suppl: 1177–1182 (2001).
35. Marin, O. & Rubenstein, J.L. A long, remarkable journey: tangential migration in the telencephalon. *Nat. Rev. Neurosci.* **2**, 780–790 (2001).
36. Corbin, J.G. *et al.* Regulation of neural progenitor cell development in the nervous system. *J. Neurochem.* **106**, 2272–2287 (2008).
37. Flames, N. *et al.* Delineation of multiple subpallial progenitor domains by the combinatorial expression of transcriptional codes. *J. Neurosci.* **27**, 9682–9695 (2007).
38. Choi, G.B. *et al.* Lhx6 delineates a pathway mediating innate reproductive behaviors from the amygdala to the hypothalamus. *Neuron* **46**, 647–660 (2005).
39. Molnar, Z. & Butler, A.B. The corticostriatal junction: a crucial region for forebrain development and evolution. *Bioessays* **24**, 530–541 (2002).
40. Waclaw, R.R. *et al.* The zinc finger transcription factor Sp8 regulates the generation and diversity of olfactory bulb interneurons. *Neuron* **49**, 503–516 (2006).
41. Stoykova, A., Fritsch, R., Walther, C. & Gruss, P. Forebrain patterning defects in Small eye mutant mice. *Development* **122**, 3453–3465 (1996).
42. Toresson, H., Potter, S.S. & Campbell, K. Genetic control of dorsal-ventral identity in the telencephalon: opposing roles for Pax6 and Gsh2. *Development* **127**, 4361–4371 (2000).
43. Tole, S., Remedios, R., Saha, B. & Stoykova, A. Selective requirement of Pax6, but not Emx2, in the specification and development of several nuclei of the amygdaloid complex. *J. Neurosci.* **25**, 2753–2760 (2005).
44. Gorski, J.A. *et al.* Cortical excitatory neurons and glia, but not GABAergic neurons, are produced in the Emx1-expressing lineage. *J. Neurosci.* **22**, 6309–6314 (2002).
45. Nery, S., Fishell, G. & Corbin, J.G. The caudal ganglionic eminence is a source of distinct cortical and subcortical cell populations. *Nat. Neurosci.* **5**, 1279–1287 (2002).
46. Marin, O., Anderson, S.A. & Rubenstein, J.L. Origin and molecular specification of striatal interneurons. *J. Neurosci.* **20**, 6063–6076 (2000).
47. Xu, Q., Tam, M. & Anderson, S.A. Fate mapping Nkx2.1-lineage cells in the mouse telencephalon. *J. Comp. Neurol.* **506**, 16–29 (2008).
48. Remedios, R. *et al.* A stream of cells migrating from the caudal telencephalon reveals a link between the amygdala and neocortex. *Nat. Neurosci.* **10**, 1141–1150 (2007).
49. Garcia-Lopez, M. *et al.* Histogenetic compartments of the mouse centromedial and extended amygdala based on gene expression patterns during development. *J. Comp. Neurol.* **506**, 46–74 (2008).
50. Corbin, J.G., Gaiano, N., Machold, R.P., Langston, A. & Fishell, G. The Gsh2 homeodomain gene controls multiple aspects of telencephalic development. *Development* **127**, 5007–5020 (2000).